J. Res. Inst. Catalysis, Hokkaido Univ., Vol. 24, No. 1, pp. 1 to 26 (1976)

ON PHOTOELECTROCHEMICAL KINETICS

By

J. O'M. BOCKRIS*), S. U. M. KHAN*)
and K. UOSAKI*)

(Received December 17, 1975)

Abstract

The phenomenology and defects in former models are presented.

A model for obtaining the current-potential and current-frequency relation is set up. The interaction energy of a photoelectron with a molecule adsorbed on the electrode is obtained by considering the Coulomb interaction between the electron and the +ve and −ve centres of the water dipole. Coulomb and Born interactions are accounted for. The barrier height is evaluated in terms of these potential energies.

The equation for the current in photoemission accounts for the reflective properties of the metal, electron-phonon and electron-electron scattering, the excitation probability from photon-electron interactions, the probability of barrier penetration and the presence of two kinds of acceptor states in solution.

The equation is evaluated quantitatively and gives an absolute value of the photocurrent. It shows that (photo-current)$^{2/5}$ should be linear with the electrode potential. The threshold energy evaluated for Hg is in fair agreement with experiment. The ability of the equation to represent the 5/2 law is insensitive to the change of barrier parameters.

The photo-current is non-Tafelian because the incident photons in the range of >3.0 eV lift the photo-electrons to energies above the ground state of the H_3O^+ vibrational-rotational states: no distribution law for their presence is effective. The electrons of the dark current emit at lower energies and are predominently accepted by the (exponentially distributed) H_3O^+ states, and this fact leads to Tafel-like relations.

1. Introduction

Photoeffects at electrodes have been studied from early times[1,2,3]. Most of the work before 1950 was complicated by a lack of definition of the state of the electrode.

Since the mid-1960's, reliable publications involving sophisticated techniques have appeared[4~8]. Two models exist. In one, the effect of light upon the electrode reaction originates in the absorption of photons by adsorbed molecules or radicals which are taking part in the rate determin-

*) School of Physical Sciences, The Flinders University of South Australia, Bedford Park, South Australia, 5042.

ing step[3,9]. Thus, HEYROVSKÝ[5] considers the photoeffect to be associated with decomposition (by light) of a surface charge transfer complex formed by solvent or solute molecules. The absorption of a light quantum breaks a bond; bonding electrons are transferred to the electrode (anodic photocurrent) or to the adsorbed molecules, which migrate away from the electrode surface (cathodic photocurrent).

The second mechanism concerns light induced electron emission from the electrode. Experimental facts are shown in Table 1, and compared with predictions for two theories which have expressed this mechanism mathematically.

TABLE 1. Models of photoelectrochemical effects

Photoelectrochemical phenomena	Experimental facts	Models	
		HILLSON and RIDEAL[3] (1949)	BRODSKII *et al.*[13] (1968)
1. Mechanism considered by different models.		Activation of adsorbed radicals by light is rate determining step.	Used photoemission of electron to electrolyte as rate determining step. Quantum mechanical flux expression used. Schrödinger equation solved to get wave function for electron, ψ, but only image interaction used in potential energy term.
2. Photocurrent I_p and potential V.	$(I_p)^{2/5} \propto V$[4,6~8]	$\log I_p \propto V$	$(I_p)^{2/5} \propto V$
3. Photocurrent I_p and light energy $h\nu$.	$(I_p)^{2/5} \propto h\nu$[8]	$\log I_p \propto h\nu$	$(I_p)^{2/5} \propto h\nu$
4. Threshold potential V_0 and light energy $h\nu$.	$V_0 \propto h\nu$[4,6~8]	No connection between Fermi level electrons in metal and activation.	$V_0 \propto h\nu$

Theories connected with the photoemission mechanism are more consistent with experimental facts than those associated with activation of species on the electrode surface. Nevertheless, there must be some cases where the absorption of light by surface radicals, or charge transfer complexes, is important, because light does sometimes cause acceleration of an anodic electrode reaction, in principle possible by the stimulated photoemission of an electron from species in the solution.

FOWLER[10] deduced a law for the photoemission current at a metal-

vacuum interface, according to which the photoemission current is proportional to the square of the radiation frequency. The experimental photocurrent[11,12] at a metal-vacuum interface for most metals usually follows this law ($I_p^{1/2} \propto h\nu$). However, recent experimental investigations[4,6~8] show that cathodic photocurrents at metal-electrolyte interfaces do not obey the square law, but rather are proportional to the 5/2th power of radiation frequency or electrode potential (5/2 law).

Two theories[13,14] have been put forward to explain the dependence of photocurrent, I_p, on potential ($I_p^{2/5} \propto V$). Both lead to an interpretation of the 5/2 law, but they do so either with neglect of the effect of the structure of the interface[13], or by consdidering it unrealistically for the time domain of electron transfer[14].

2. Quantitative Discussion of BRODSKII's Model (1968)

Direct photoemission of an electron is considered to be the rate determining step in this model[13]. An expression for the photocurrent is derived from a usual quantum mechanical expression for flux, but the wave function used in the expression for the flux was obtained by solving SCHRÖDINGER's equation in which it was assumed that the only potential energy experienced by the escaping electron was the image potential of the electrons in the metal. This choice of potential energy is the difficulty of BRODSKII's model, because at the short times involved there is no image potential between metal and electron (see section 3(d)), and because other sources of potential energy (apart from that of the image energy) are experienced by an electron during its escape from a metal through the interface[15]. Another difficulty of the BRODSKII model is that its principal approximations involved the use of the static dielectric constant of the solution, whereas in fact an optical dielectric constant should be used for the time domain of electron emission from the electrode to solution. Use of an optical value for the dielectric constant, ε_{op}, in BRODSKII's photocurrent expression[13] shows that, then, it does not give the 5/2 law.

3. The Present Model (Qualitative)

The photoemission of an electron from the metal to acceptor states in the electrolyte across the potential energy barrier at the metal-solution interface is taken to be the rate determining step. The potential energy barrier was constructed by considering the path of a hypothetical electron which would move classically over the top of the barrier to a defined acceptor state. The following considerations have been made in construct-

ing the potential energy barrier for the electron at the interface.

(a) *The Interaction energy of an electron with the water molecules adsorbed on the electrode*

During the transfer of an electron across the electrode-electrolyte interface, an important interaction will be with the positive and the negative centres of adsorbed water molecules on the electrode surface.

This *classical* interaction energy can be calculated as a function of distance from the metal by considering the Coulomb interaction of the electron with the positive and the negative centres of the adsorbed water molecules during its transit across them. This Coulomb interaction in the first water layer, U_{H_2O}, can be obtained using the relation[16]

$$U_{H_2O} = \begin{cases} -\dfrac{Ze_0^2}{R}\left[\dfrac{3}{2} - \dfrac{1}{2}\dfrac{r^2}{R^2}\right] & 0 \leqslant r \leqslant R \\ -\dfrac{Ze_0^2}{r}, & r \geqslant R \end{cases} \qquad (1)$$

where Z is the charge on the positive or the negative centre (*i. e.* the hydrogen or oxygen atom) respectively, e_0 is the electronic charge, R is the radius of the sphere (*i. e.* of the hydrogen or oxygen atoms), which is considered to have a uniform distribution of charge Ze_0, and r is the distance from the centre of the sphere (Fig. 1 a).

(b) *Coulomb Interaction*

When a photo-ejected electron leaves the metal surface, it experiences the Coulombic attraction and repulsion from all ions in the outer HELMHOLTZ plane (OHP), and their electrical images in the metal at an optical frequency. Equation (2) represents the Coulomb energy of these interactions*).

$$U_{\text{coulomb}} = U_1 + U_2 + U_3 + U_4 = -\frac{e_0^2}{(d-x)\varepsilon_{op}} + \frac{e_0^2}{(d+x)\varepsilon_{op}} - \frac{2e_0^2}{\varepsilon_{op}} \times \sum_{n=1}^{\infty} n\left[\frac{1}{[(d-x)^2+n^2R_1^2]^{1/2}} - \frac{1}{[(d+x)^2+n^2R_1^2]^{1/2}}\right] \qquad (2)$$

where U_1 = the Coulomb interaction energy between the emitting electron and the central ion in the OHP; U_2 = the Coulomb interaction energy between the image of the central ion in the metal electrode and the emitting electron; U_3 = the coulomb interaction energy between the emitting electron and the ions on the rings around the central ion in the OHP;

*) This is deduced in a similar way as eq. (7.139) by BOCKRIS and REDDY[17].

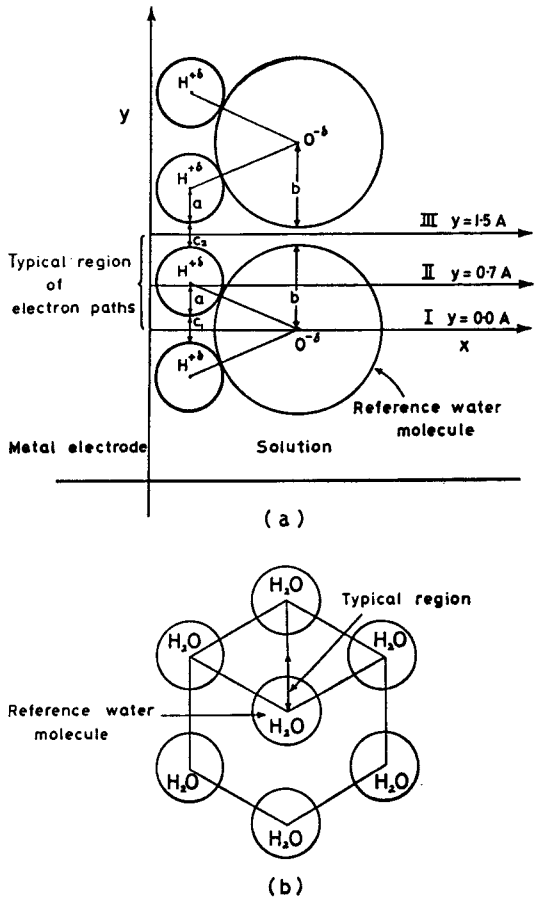

Fig. 1. The Schematic model used for the estimation of the Coulomb interaction energy of electron with the $+ve$ and $-ve$ centres of the water molecules adsorbed on the electrode surface.

(a) Shows typical region of electron paths using two water molecules.

(b) Shows hexagonal arrays of six water molecules.

and U_4 is the corresponding interaction energy with images of the ions of the rings in the metal electrode; R_1 is the average distance between the ions in the OHP depending on its coverage and determined using $R_1=4r_1/(\pi\theta)^{1/2}$, where θ is the coverage of ions in the OHP, r_1 is the radius of the ions, and n is the number of rings around the central ion (Fig. 2).

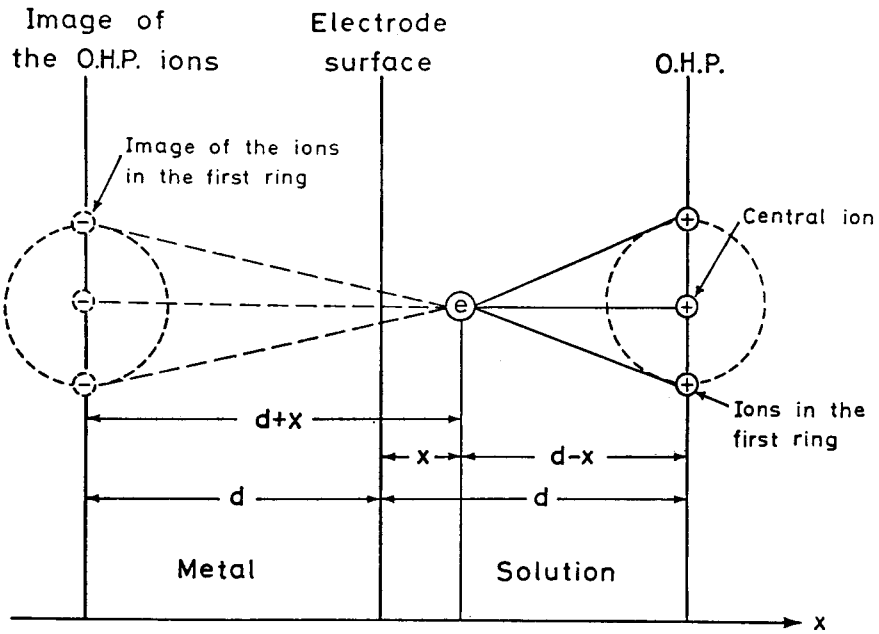

Fig. 2. The schematic model used for the estimation of the Coulomb interaction energy between the emitting electron (from the metal surface) and the ions in the outer Helmholtz plane and their images in the metal.

(c) *Optical Born Energy of the Electron*

It is more difficult to evaluate the potential energy of the electron with the second layer from the electrode than from the first, for the structure of water here is extremely heterogeneous. Hence, we follow previous authors[18,19,20] in considering the second layer of solvent molecules into the bulk from the electrode as a continuum. Thus, when the electron enters the second water layer after crossing the first structured water layer, it derives some energy from the optical Born energy of the continuum dielectric. This contribution, $U_{\text{opt.Born}}$ has been estimated by considering the charging of the electron cavity, *i. e.*,

$$U_{\text{opt.Born}} = -\frac{e_0^2}{2r_c}\left[1-\frac{1}{\varepsilon_{\text{op}}}\right] \qquad (3)$$

where r_c is the radius of electron cavity. The latter term has been used here following the SCF calculations of FUEKI *et al.*[21]

(d) *Image Interaction*

The photoejected electron does not interact with its image in the

metal since the relaxation time of the electrons within the metal conduction band is usually 10^{-14} sec, (for Hg$\sim 10^{-15}$ sec)[22] *i. e.* longer than the electron transfer time across the interface *i. e.*$\sim 10^{-16}$ sec.*) MARGENAU *et al.*[23] first showed that image forces were effective only for slowly moving charges. Although earlier GOMER[24] accounted for the image forces in electron exit calculation, more recently they have been neglected in such calculations[25,26].

4. The Height of the Potential energy Barrier at the Interface

The potential energy of interaction experienced by an electron when

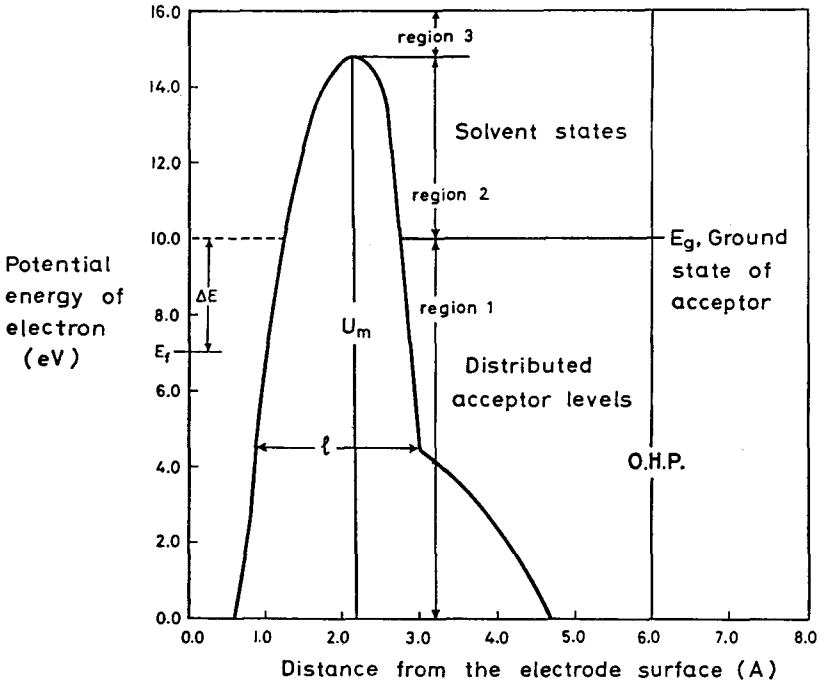

Fig. 3. A schematic diagram of the potential energy barrier for electron transfer from a mercury electrode (Φ=4.5 eV and E_f=7.0 eV) to acceptors in the electrolyte at the outer Helmholtz plane (6 A from the electrode surface).

*) Considering electron energy at Fermi level of Hg electrode as 7.0 eV the velocity of electron becomes $v=\sqrt{\frac{2E}{m}}=1.5\times10^{-8}$ cm/sec. Hence, the time required to tunnel a distance of$\sim$5 A at the interface is $t=\frac{5\times10^{-8}}{1.5\times10^{8}}=3.3\times10^{-16}$ sec.

it is in the first structured water layer is given (Fig. 3) from eqs. 1 and (2) as

$$U_{\text{Total}} = U_{H_2O} + U_{\text{coulomb}} \qquad (4)$$

Hence, the height of the potential energy barrier at the interface measured with respect to the bottom of the conduction band of the metal is given by

$$U_m = E_f + \Phi + U_{\text{Total, maximum value}}, \qquad (5)$$

where E_f = the Fermi energy of the electron in the metal;
Φ = the work function of the metal.

5. The Energy of an Electron in the Ground State of an H_3O^+ Ion

To find the energy of an electron in the ground state of H_3O^+ near an electrode in solution, one brings an electron from vacuum to H_3O^+ in solution forming: $H_2O\cdots H$ near the electrode surface.

The energy change in this process can be written as

$$-L_0 - J + R + A,$$

where L_0 is the solvation energy of H^+ in water, J the ionization energy of the H-atom, R the repulsive interaction for the $H\cdots H_2O$ distance at the moment of arrival of the electron, and A is the attractive $M\cdots H$ interaction at that moment.

On uses values[27,28] $L_0 = -11.4$ eV; $J = 13.6$ eV; $R = 1.0$ eV and $A = -0.3$ eV. Thus, $-L_0 - J + R + A = -1.5$ eV. Hence, the difference in potential energy between the electron in the ground state of H_3O^+ and that at the Fermi level of the electrode (Hg) is (Fig. 3)

$$\Delta E = -1.5 \text{ eV} + \Phi = -1.5 + 4.5 = 3.0 \text{ eV} \qquad (6)$$

where Φ is the work function*) of the Hg-electrode. The ΔE value indicates that the energy of the electron in the ground state of the acceptor (H_3O^+ ion) is 3.0 eV above the Fermi level of the mercury electrode and the ground state energy of the acceptor, E_g, is

$$E_g = E_f + \Delta E = 7.0 \text{ eV} + 3.0 \text{ eV} = 10.0 \text{ eV} \qquad (7)$$

above the bottom of the conduction band of mercury (Fig. 5).

*) The value of Φ is not the hypothetical value of Φ in solution but the Φ for the metal-vacuum interface. Thus, the changes caused by the work done to expel an electron from the metal to states in the solution has been allowed for in the calculation of the interaction of the electron with the water layer on the electrode surface (eq. 1).

In the estimation of the ground state energy of the acceptor (H_3O^+ ion) we have considered that the Fermi level of the mercury electrode is not changed from its vacuum value when it is dipped into the solution, disconnected from an electric circuit, inasmuch as the Fermi energy is a bulk property of the metal, and hence E_f (vacuum)$=E_f$ (at the *p. z. c.* in contact with the solution). Thus, the Fermi energy at some *rational* potential, V, becomes

$$(E_f)_V = (E_f)_{\text{vacuum}} - e_0 V, \tag{8}$$

where V must be used with the appropriate sign.

6. Theoretically Expected Threshold for the Photocurrent

Figure 3 shows that only electrons which have an energy equal or greater than ΔE will cause emission of electrons to acceptors of electrons in the water states and not in the distributed states in H_3O^+. Detailed computations of the relative contributions of the various terms in the expression for the photocurrent, (see eq. (33)), show that the second term predominates. As this term represents the rate of electron transfer through the barrier to solvent states in the solution, it is possible to associate the threshold energy of photons as that of those which are able to increase the energy of electrons in the Fermi level to values equal to E_g. This value is 3.0 eV above the Fermi level (see section 5). (The experimental value[8] is 3.15 eV.)

7. Photoemission Current into an Electrolyte

(i) *The number of photoelectrons which reach the metal surface*

Let a monochromatic beam of photons having an energy $h\nu$ be incident upon a metal-electrode surface in the x direction of a rectangular coordinate system. Some light will be reflected, some absorbed within the metal, and some excite electrons in the metal conduction band. We calculate the following:

(a) The number of electrons per unit area and time which are excited by an incident photon of intensity I_0 at depths between x and $(x+dx)$ inside the metal from the surface. It is simple to show that this is:

$$N(x, x+dx) = I_0(1-R_f)\alpha_p e^{-\alpha_p x} dx \tag{9}$$

where R_f is the reflection coefficient of the metal and α_p is the absorption coefficient of the metal for the photon of frequency ν.

(b) The probability $P_1(E, h\nu)$ of excitation of an electron in the metal electrode to an energy state E from an energy state $(E-h\nu)$. This is given by

$$P_1(E, h\nu) \propto \rho(E)(1-f(E))\,\rho(E-h\nu)f(E-h\nu)\,\mathrm{d}E \tag{10}$$

Normalising $P_1(E, h\nu)$ to unity one gets

$$P_1(E, h\nu) = \frac{\rho(E)(1-f(E))\,\rho(E-h\nu)f(E-h\nu)\,\mathrm{d}E}{\int_{h\nu}^{\infty} \rho(E)(1-f(E))\,\rho(E-h\nu)f(E-h\nu)\,\mathrm{d}E}$$

$$= \frac{1}{Q}\rho(E)(1-f(E))\,\rho(E-h\nu)f(E-h\nu)\,\mathrm{d}E \tag{11}$$

$$i.\,e. \quad Q = \int_{h\nu}^{\infty} \rho(E)(1-f(E))\,\rho(E-h\nu)f(E-h\nu)\,\mathrm{d}E \tag{12}$$

where Q is the normalisation factor, $\rho(E)$ is the density of elctron states, $(1-f(E))\,\rho(E)$ the number of vacant states at energy E, $\rho(E-h\nu)$ the density of state corresponding to energy $(E-h\nu)$ and $f(E-h\nu)$ is the Fermi distribiution of electrons in the metal corresponding to the energy $(E-h\nu)$.

(c) The probabilities of photo-excited electrons from within the bulk of the metal reaching the surface at different angles without suffering an inelastic electron-phonon ; and the electron-electron scattering event. Each probability is given by (Fig. 4):

$$P_2 = \exp\left[-\frac{x}{L_s \cos\theta \cos\phi}\right] \tag{13}$$

where L_s is the electron-phonon or electron-electron scattering length. Thus, the number of electrons, N (per cm^2 per sec) which absorb photons at a depth between x and $(x+\mathrm{d}x)$, and which reach the surface without undergoing inelastic scattering is given from eqs. (9) and (13) by :

$$N = \int_0^{\infty} N(x, x+\mathrm{d}x) \exp\left[-\frac{x}{L_s \cos\theta \cos\phi}\right]\mathrm{d}x$$

$$= \int_0^{\infty} I_0(1-R_f)\,\alpha_p \exp\left[-\left[\alpha_p + \frac{1}{L_s \cos\theta \cos\phi}\right]x\right]\mathrm{d}x$$

$$= I_0(1-R_f)\frac{\alpha_p}{\alpha_p + \dfrac{1}{L_s \cos\theta \cos\phi}} \tag{14}$$

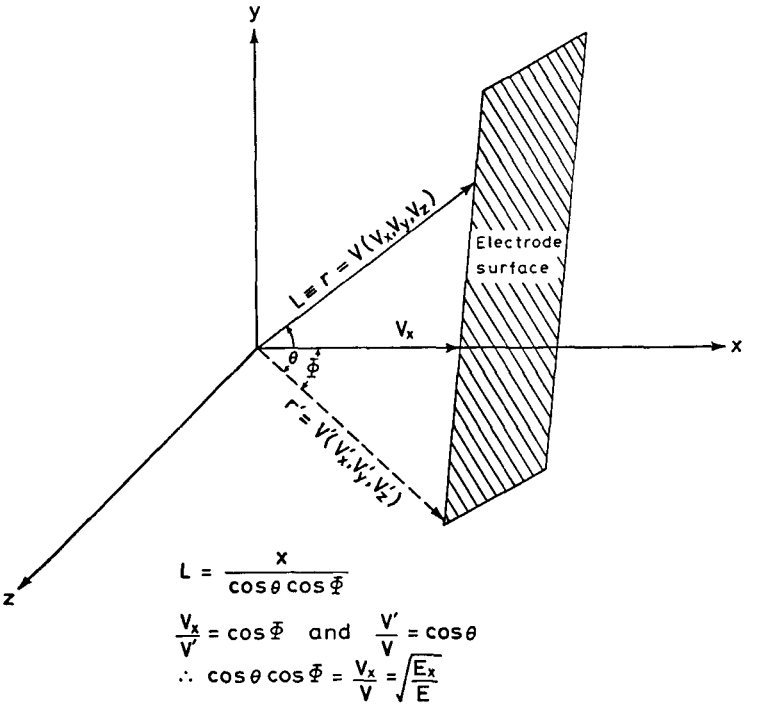

Fig. 4. Vectorial representation of the angular distribution of the electrons which move towards the metal surface from within the bulk when stimulated by light.

In eq. (14), L_s is either the electron-electron or the electron-phonon scattering length. In some metals, the electron-phonon length is dominant, and, in others, it is the electron-electron scattering length. In the present phenomena (electron energy range 2.5 to 11.0 eV for the metal Hg) electron-phonon scattering length is dominant[22]. The factor $\cos\theta \cos\phi$ has come into expression (14) to account for the three dimensional angular orientation of the outgoing electron towards the surface. This angular factor can be expressed in terms of the total velocity (v), and the x component of velocity (v_x), and thus also in terms of total energy, E (Fig. 4). It is evident that (Fig. 4)

$$\cos\theta \cos\phi = \frac{V_x}{V(x, y, z)} = \frac{E_x^{1/2}}{E^{1/2}} \tag{15}$$

From eqs. (14) and (15) one gets

$$N = I_0(1-R_f)\frac{1}{1+\frac{\alpha_s}{\alpha_p}\sqrt{\frac{E}{E_x}}} \tag{16}$$

where $\alpha_s = (L_s)^{-1}$.

$$\text{Since } \frac{\alpha_s}{\alpha_p} \gg 1, \qquad N \simeq I_0(1-R_f)\frac{\alpha_p}{\alpha_s}\sqrt{\frac{E_x}{E}} \tag{17}$$

(d) The number of electrons having a velocity component perpendicular to the surface (*i. e.* parallel to the x-axis) corresponding to energy E_x and $(E_x+\mathrm{d}E_x)$. This number can be obtained from equations (11) and (17) as follows:

The number (per unit area and time) of unscattered excited electrons at any energy E_x is given from eqs. (11) and (17) (considering the x component of energy E_x) as

$$NP_1(E_x, h\nu) = \frac{I_0(1-R_f)}{Q}\frac{\alpha_p}{\alpha_s}\frac{E_x^{1/2}}{E^{1/2}} \times \rho(E_x)(1-f(E_x))\,\rho(E_x-h\nu)f(E_x-h\nu)\,\mathrm{d}E_x \tag{18}$$

Putting in the standard values of $\rho(E)$ and $1-f(E)$ one gets

$$NP_1(E_x, h\nu) = \frac{B'I_0(1-R_f)\alpha_p}{Q\alpha_s}E_x^{1/2}\left[\exp\left[\frac{E_f-E_x}{kT}\right]+1\right]^{-1} \times\left[\rho(E_x-h\nu)f(E_x-h\nu)\,\mathrm{d}E_x\right] \tag{19}$$

where $B' = 4\pi(2m)^{3/2}/h^3$.

In equation (19) we have considered the probability of having the vacant states of fraction $(1-f(E_x))$ corresponding to the x component of velocity in velocity space, *i. e.* corresponding to the energy E_x only. This is a good approximation since the factor $(1-f(E))$ is unity in most situations when $(E_x-E_f) \gg kT$.

The factor $\rho(E_x-h\nu)f(E_x-h\nu)\,\mathrm{d}E_x$ of eq. (19) is obtained by integrating $\rho(E-h\nu)f(E-h\nu)\,\mathrm{d}E$ with respect to the y and z components of energy E and this gives the number of electrons having their x component of energy, E_x, directed normal to the surface. Since energy E is a scalar quantity one prefers to do this integration in terms of velocity. The equivalent expression for $\rho(E-h\nu)f(E-h\nu)\,\mathrm{d}E$ in terms of momentum and then velocity is given by

$$\rho(E-h\nu)f(E-h\nu)\,\mathrm{d}E \equiv \frac{2}{h^3}\frac{\mathrm{d}p_x\mathrm{d}p_y\mathrm{d}p_z}{\exp\left[\frac{E-h\nu-E_f}{kT}\right]+1} = 2\left[\frac{m}{h}\right]^3\frac{\mathrm{d}v_x\mathrm{d}v_y\mathrm{d}v_z}{\exp\left[\frac{m(v_x^2+v_y^2+v_z^2)/2-h\nu-E_f}{kT}\right]+1} \tag{20}$$

Transforming in terms of polar coordinate system the integral of eq. (20) can be written as

$$\int \rho(E-h\nu)f(E-h\nu)\,\mathrm{d}E \equiv 2\left[\frac{m}{h}\right]^3 \mathrm{d}v_x \int_0^{\infty}\int_0^{2\pi} \frac{\xi\,\mathrm{d}\xi\,\mathrm{d}\theta}{\exp\left[\dfrac{m(v_x^2+\xi^2)/2-h\nu-E_f}{kT}\right]+1} \tag{21}$$

where $\xi = \sqrt{v_y^2+v_z^2}$.

After integration with respect to the y and z component, *i.* e. with respect to ξ and θ one gets

$$\rho(E_x-h\nu)f(E_x-h\nu)\,\mathrm{d}E_x \equiv \frac{4\pi kT}{m}\left[\frac{m}{h}\right]^3 \times \ln\left[1+\exp\left[\frac{E_f+h\nu-mv_x^2/2}{kT}\right]\right]\mathrm{d}v_x \tag{22}$$

Rewriting the eq. (22) in terms of energy, one gets

$$\rho(E_x-h\nu)f(E_x-h\nu)\,\mathrm{d}E_x = \frac{\pi(2m)^{3/2}}{h^3}kT \times \ln\left[1+\exp\left[\frac{E_f+h\nu-E_x}{kT}\right]\right]E_x^{-1/2}\,\mathrm{d}E_x \tag{23}$$

Thus, eq. (23) gives the number of electrons with a velocity component v_x, and $v_x+\mathrm{d}v_x$ and in terms of energy, the number of electrons in the direction x towards the surface which has the energy E_x, $E_x+\mathrm{d}E_x$. A substitution of $\rho(E_x-h\nu)f(E_x-h\nu)\,\mathrm{d}E_x$ from eq. (23) to eq. (19) and making the transformation for the presence of applied potential, V (negative for the cathodic polarization) will then give the number of photoelectrons per unit area and time which strike the surface and have energies between E_x and $E_x+\mathrm{d}E_x$. This is:

$$N_p(E_x, E_x+\mathrm{d}E_x) = \frac{I_0(1-R_f)\alpha_p\, kTB}{4Q'B\alpha_s}\left[\exp\left[\frac{E_f-e_0V-E_x}{kT}\right]+1\right]^{-1} \times \ln\left[1+\exp\left[\frac{E_f+h\nu-e_0V-E_x}{kT}\right]\right]\mathrm{d}E_x \tag{24}$$

where

$$B = \left[\frac{4\pi(2m)^{3/2}}{h^3}\right]^2 \tag{25}$$

$$Q'B = Q \tag{26}$$

Equation (24) represents the number of photoelectrons at any energy E the resolved velocity components v_x of which are normal to the surface and which can reach the surface without scattering.

The quantity Q' defined in eq. (26) is obtained from eq. (12) with the use of standard values of $\rho(E)$, $\rho(E-h\nu)$, $f(E)$ and $f(E-h\nu)$ as,

$$Q' = \int_{h\nu}^{\infty} E^{1/2}(E-h\nu)^{1/2}\left[\exp\left[\frac{E_f-E}{kT}\right]+1\right]^{-1} \times \left[\exp\left[\frac{E-h\nu-E_f}{kT}\right]+1\right]^{-1} dE \tag{27}$$

(ii) *The number of photoelectrons per unit area which pass through the barrier to acceptors in solution*

The photocurrent is proportional to the number of photoelectrons which can reach the surface without scattering, $N_p(E_x, E_x+dE_x)$, the probability of tunneling of these through the potential barrier at the interface, $P_T(E_x)$ and the probability of the presence of acceptor states, $G(E_x)$, of the same energy as that of an emitting electron. Hence, the photocurrent (amps cm^{-2}) can be expressed as

$$I_p = e_0 \frac{C_A}{C_T}\int_{h\nu}^{\infty} N_p(E_x, E_x+dE_x)\,P_T(E_x)\,G(E_x)\,dE_x \tag{28}$$

where C_A and C_T are respectively the total number of acceptors per unit area of the outer Helmholtz plane (OHP) and the total number of sites per unit area of OHP; $P_T(E_x)$ is the W. K. B. tunneling probability of electron across the potential barrier of height U_m and width l, *i. e.*,

$$P_T(E_x) = \exp\left\{-\frac{\pi^2 l}{h}\left[2m(U_m-E_x)\right]^{1/2}\right\} \tag{29}$$

and $G(E_x)$ represents the population of vibrational-rotational states of acceptor in solution*) at different energies E_x, *i. e.*,

$$G(E_x) = \exp\left\{-\beta(E_g-E_x)/kT\right\} \tag{30}$$

Using eq. (24) in eq. (28) one gets

$$I_p = \frac{e_0 A'}{Q'}\frac{C_A}{C_T}\int_{h\nu}^{\infty}\left[\exp\left[\frac{E_f-e_0V-E_x}{kT}\right]+1\right]^{-1}$$

*) This BOLTZMANN function is an appropriate function for the acceptors in solution since their energies are smoothed out. The factor β is the symmetry factor.

$$\times \ln\left[1+\exp\left[\frac{E_f+h\nu-e_0V-E_x}{kT}\right]\right]P_T(E_x)\,G(E_x)\,dE_x \qquad (31)$$

where

$$A' = \frac{I_0(1-R_f)\,\alpha_p\,kT}{4\alpha_s} \qquad (32)$$

For the practical evaluation of the photocurrent one can write the integral (31) in three parts for the three regions of the barrier (Fig. 3), *i. e.*

$$\begin{aligned} I_p = \frac{e_0A'}{Q'}\frac{C_A}{C_T}\Bigg\{ & \int_{h\nu}^{E_g}\left[\exp\left[\frac{E_f-e_0V-E_x}{kT}\right]+1\right]^{-1} \\ & \times \ln\left[1+\exp\left[\frac{E_f+h\nu-e_0V-E_x}{kT}\right]\right]P_T(E_x)\,G(E_x)\,dE_x \\ & + \int_{E_g}^{U_m}\left[\exp\left[\frac{E_f-e_0V-E_x}{kT}\right]+1\right]^{-1} \\ & \times \ln\left[1+\exp\left[\frac{E_f+h\nu-e_0V-E_x}{kT}\right]\right]P_T(E_x)\,dE_x \\ & + \int_{U_{in}}^{\infty}\left[\exp\left[\frac{E_f-e_0V-E_x}{kT}\right]+1\right]^{-1} \\ & \times \ln\left[1+\exp\left[\frac{E_f+h\nu-e_0V-E_x}{kT}\right]\right]dE_x\Bigg\} \end{aligned} \qquad (33)$$

The first integral of the eq. (33) gives the contribution of photocurrent from the photoelectrons which tunnel through the barrier to the distributed acceptor states corresponding to the vibrational rotational energy of an acceptor, H_3O^+.

The second integral of the eq. (33) gives the contribution of photocurrent from the photoelectron which tunnels through the barrier and goes to the solvent states. The major contribution for photon energies greater than 3.0 eV and not more than about 10.0 eV comes from such electrons. After emission into the solution these high energy electrons lose their kinetic energy by inelastic collision with the bulk water molecules and ultimately get accepted by the solvent molecules.

The third integral of eq. (33) gives contribution to the photocurrent from the photoelectron which can go over the barrier.

8. The Present Model (Quantitative)

(a) *Quantitative estimation of the interaction energy of an electron with the adsorbed water molecules*:

The quantitative estimation of the interaction energy of an electron with the positive and negative centres of the adsorbed water molecules can be made using the eq. (1). A hexagonal arrangement of the adsorbed water molecules around a reference water molecule has been considered (Fig. 1 b) and thus a region from the centre of the reference water molecule to the centre in between the reference molecule and the adjacent water molecule can be considered as the typical region such that all other regions in the surface become equivalent to this typical region with respect to interaction with the electron. In this typical region, three water molecules are involved in the interaction with the electron (during its passage) along with the reference one. In Fig. 1 a only two water molecules have been shown, but the situation considered is shown in Figs. 1 a and 1 b.

To calulate U_{H_2O} from eq. (1), the charge Z on each hydrogen atom has been taken as $Z=+0.19$ and on oxygen atom as $Z=-0.38$[29]. The radius of hydrogen atom has been taken as the Bohr radius, *i. e.* 0.53 A and for the oxygen atom as 0.85 A [$=(1.38-0.53)$ A] where 1.38 A is the radius of water molecule. In Fig. 1 a, the lengths a and b represent the radius of hydrogen and oxygen atom respectively. The length c_1 is the distance between the edges of the two H-atoms in a water molecule and which is equal to 0.23 A (calculated from the values of the distance between the centres of the H and the O-atoms and the angle between H, O and H in a water molecule). The length c_2 is the distance between two adsorbed water molecules on an electrode surface$=0.14$ A (calculated considering the coverage of 0.9 for water molecules on the electrode surface. To find the distance r between the centres of hydrogen and oxygen atom and the electron for its various positions across the adsorbed water layer, the values of a, b, c_1 and c_2 have been used. The Coulomb energy, U_{H_2O}, has been calculated for the various positions of electron from the electrode surface to the end of the first water layer in the direction perpendicular to surface. Similar calculations have been carried out for different paths of the electron along the surface (*i. e.* parallel to the surface) from the centre of the reference water molecule to the centre in between the reference and the adjacent water molecules. These calculations have been carried out using eq. (1) and the computer DEC system-10. Since the variation of the interaction energies of an electron for the different paths in the typical region is

not significant, we have averaged the interaction energies over the different paths. A justification for this is shown in Fig. 5 where the potential energy-distance relations for 3 paths are shown. The average interaction energies of an electron with the adsorbed water molecules as a function of distance from the metal surface up to the end of the first water layer are shown in Table 2. The barrier model with these average interaction energy along with other interactions from eq. (4) is shown in Fig. 3.

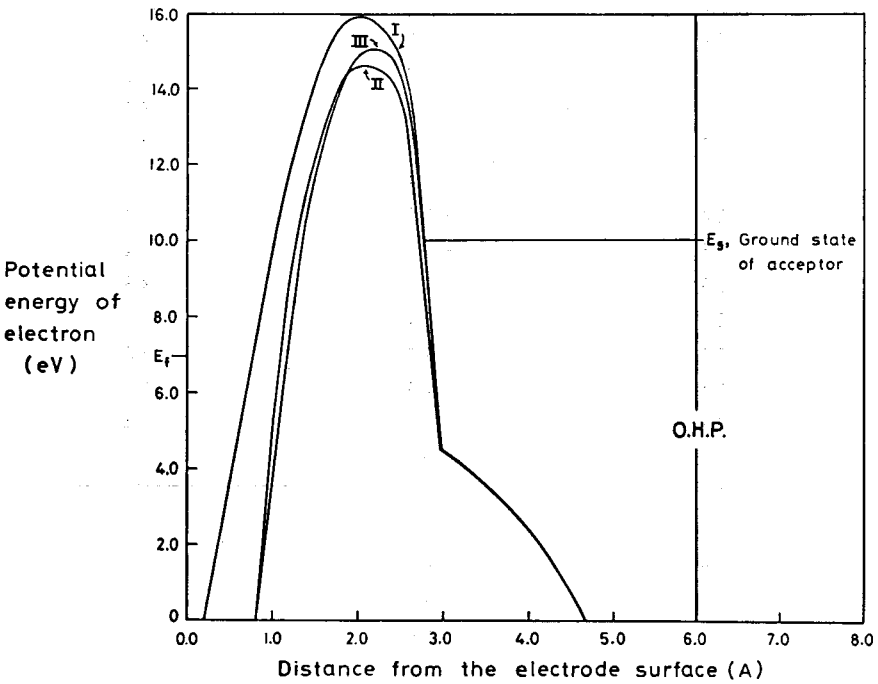

Fig. 5. Schematic diagrams of potential energy barrier for three typical paths of electron as shown in Fig. 1. I, for the electron path when $y=0.0$ A. II, for the electron path when $y=0.7$ A. III, for the electron path when $y=1.5$A.

(b) *Coulomb Interaction Potential*

The Coulomb interaction potential was calculated using expression (2) with the help of Computer DEC system-10. The distance, d, between the outer Helmholtz plane and the metal surface was taken as 6 A (Fig. 2) and the distance R between two solvated ions on OHP as 10 A for the coverage $\theta=0.1$ for the H_3O^+ ion.

The computed values of the Coulomb potential of the electron at various distances from the metal surface are tabulated in Table 2.

TABLE 2. The values of Coulomb potential at various distances of electron from metal (eq. 2) and the interaction energy of electron with the adsorbed water molecules (eq. 1)

Distance from metal in A	Coulomb potential $U_{coulomb}$ in eV	U_{H_2O} in eV
0.0	− 0.0	−13.0
0.2	− 0.2	−13.02
0.4	− 0.5	−14.6
0.6	− 0.7	−14.9
0.8	− 0.9	− 8.2
1.0	− 1.2	− 4.2
1.2	− 1.4	− 1.1
1.4	− 1.6	1.4
1.6	− 1.9	3.4
1.8	− 2.1	4.8
2.0	− 2.4	5.6
2.2	− 2.7	6.0
2.4	− 2.9	5.9
2.6	− 3.2	5.4
2.8	− 3.5	4.7
3.0	− 3.8	
3.2	− 4.2	
3.4	− 4.5	
3.6	− 4.9	
3.8	− 5.4	
4.0	− 5.9	
4.2	− 6.5	
4.4	− 7.2	
4.6	− 8.0	
4.8	− 9.1	
5.0	−10.6	
5.2	−12.7	
5.4	−16.2	

(c) *The Born Energy of the Electron*

Using equantion (3), the contribution of the Born energy of an electron cavity (utilising the cavity radius of 1.0 A, calculated by FUEKI[21]) was computed to be $U_{opt.Born}=3.2$ eV.

(d) *The Barrier Height*

The barrier height*) with respect to the bottom of the conduction band of the metal was esitmated using the eq. (5) and from Fig. 3.

(e) *The Barrier Width*

Taking into account the considerations mentioned in (a), (b), (c) and (d), we have construced the barrier, and the corresponding schematic diagram is shown in Fig. 3. The barrier width is 2.2 A in its most important part (Fig. 3). The lower part of the barrier is wide and the contribution to the photocurrent from such a region is negligible.

9. Computation of the Photocurrent

Photocurrents at the metal-solution interface were computed at rational potentials, V, by numerical integration of expression (33) using the computer

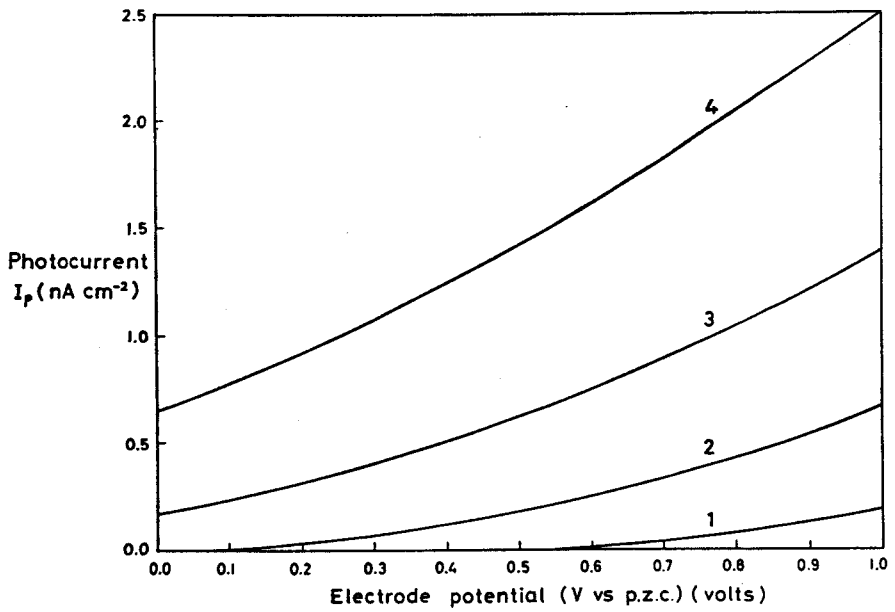

Fig. 6. The dependence of the photocurrent on electrode potential for electron transfer from a mercury electrode to acceptors in the electrolyte for different incident photon energies, $h\nu$. Curve 1, for $h\nu=2.5$ eV. Curve 2, for $h\nu=3.0$ eV. Curve 3, for $h\nu=3.5$ eV. Curve 4, for $h\nu=4.0$ eV.

*) The precise value of the barrier height turns out to be unimportant since variation of even as much as ± 1.0 eV does not affect the applicability of the 5/2 law and the calculated threshold energy is affected by less than 0.1 eV (Fig. 8). But it is important for the absolute value of I_p.

DEC system-10. Figure 6 shows the calculated photocurrents for different incident light energies, $h\nu$.

The photocurrent I_p is given in absolute units (nanoamps cm^{-2}), *i. e.* an absolute calculation, and not in arbitrary units, as in previous models[13,14]. The incident light intensity I_0 used in this calculation is 10^{15} quanta cm^{-2} sec^{-1} [3].

The constant A' of eq. (33) has been computed from eq. (32) using reflection coefficient R_f (values for Hg-electrode) and values of the α_p for different radiation energies $h\nu$. The parameter α_p has been calculated using $\alpha_p = \frac{4\pi K_p}{\lambda_p}$, where K_p is the extinction coefficient of the photon[30] (Table 3). The parameter α_s has been calculated for the energy of electrons corresponding to the Fermi energy of mercury. Since in mercury the electron-phonon scattering length is smaller than the electron-electron scattering length, we have calculated α_s using the relation $\alpha_s = (V_F \tau)^{-1}$, where V_F is the electron velocity corresponding to the Fermi energy and τ is the relaxation time of the Fermi level electrons. The electron-phonon scattering is almost independent of the energy of the electron[22,31,32]. We have not taken into account its energy dependence, since this is much less than the temperature dependence[31] *i. e.* at room temperature, α_s (electron-phonon) may be considered constant with change of electron energy (see Table 3). The $\frac{C_A}{C_T}$ value was taken as unity for the part of eq. (33) in which electrons are being donated to the solvent and 0.1 when the acceptor is H_3O^+.

The electron-electron scattering length is appreciably dependent on the energy of the electron, but this scattering length is longer than the electron-phonon scattering length in mercury, and hence electron-electron scattering length has not been used here.

TABLE 3. The values used to calculate the constant A′ of equation (33) used for the computation of photocurrent for different photon energies, $h\nu$

Photon energy $h\nu$ (eV)	Reflection coefficient of photon in Hg-metal, R_f [30]	Electron-phonon scattering length in Hg-metal, $L_s = (\alpha_s)^{-1}$ (cm)	Absorption coefficient of phonon in Hg-metal α_p (cm^{-1})[30]	The value of constant A′ used in equation (33) (cm^{-2} sec^{-1} ergs)
2.5	0.747	1.105×10^{-7}	9.69×10^5	0.27
3.0	0.731		9.99×10^5	0.30
3.5	0.705		9.4×10^5	0.31
4.0	0.663		8.94×10^5	0.34

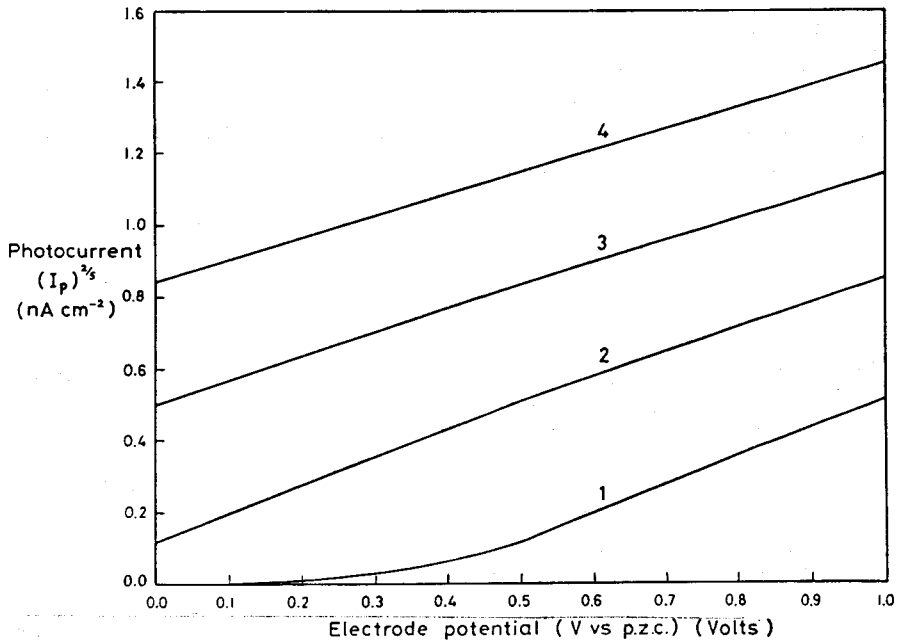

Fig. 7. The dependence of 2/5th power of the photocurrent on electrode potential for electron transfer from a mercury electrode to acceptors in the electrolyte for different incident photon energies, $h\nu$. Curve 1, for $h\nu=2.5$ eV. Curve 2, for $h\nu=3.0$ eV. Curve 3, for $h\nu=3.5$ eV. Curve 4, for $h\nu=4.0$ eV.

The photocurrent $(I_p)^{2/5}$ against potential, V, has been plotted (Fig. 7) for different incident light energies $h\nu$. There is linearity for a potential change from the potential of zero charge (*p. z. c.*) for at least one decade.

The threshold energy, $h\nu_0$, for photoemission into the electrolyte was determined by plotting $(I_p)^{2/5}$ against potentials, V (Fig. 7), and extrapolating to $(I_p)^{2/5}=0$. The extrapolated potential, corresponding to $(I_p)^{2/5}=0$ is the threshold potential, V_0. The threshold photon energy $h\nu_0$ was obtained from the relation

$$h\nu_0 = h\nu - e_0 V_0 \tag{34}$$

where $h\nu$ is the incident photon energy. In each calculation to determine the photocurrent, the ground state energy E_g of the acceptor H_3O^+ was taken to be 10.0 eV with respect to the bottom of the conduction band, and it is 3.0 eV above the Fermi level of the Hg-electrode. The results of the extrapolated value of the threshold energy from the plots of Fig. 7 are in good agreement with the theoretically expected threshold (Table 4).

The linear behaviour of the plot of $(I_p)^{2/5}$ against potential V, and agreement of the extrapolated threshold light energy $h\nu_0$ with the experimental one[8], and also with the theoretically expected threshold energy (see Section 6 and Table 4) confirms the consistence of the model with experiment and with the 5/2 law for the photocurrent.

TABLE 4. The results to compare the threshold energies $h\nu_0$ (extrapolated) with the expected and experimental threshold energies at different photon energies $h\nu$

Photon energy $h\nu$ in eV	Threshold energy $h\nu_0$ (extrapolated) in eV from figure 7 (from eq. (33))	Theoretically expected threshold (see Section 6) in eV	Experimental threshold energy in eV[8]
2.5	2.9	3.0	
3.0	2.8	3.0	3.15
3.5	2.8	3.0	
4.0	2.7	3.0	

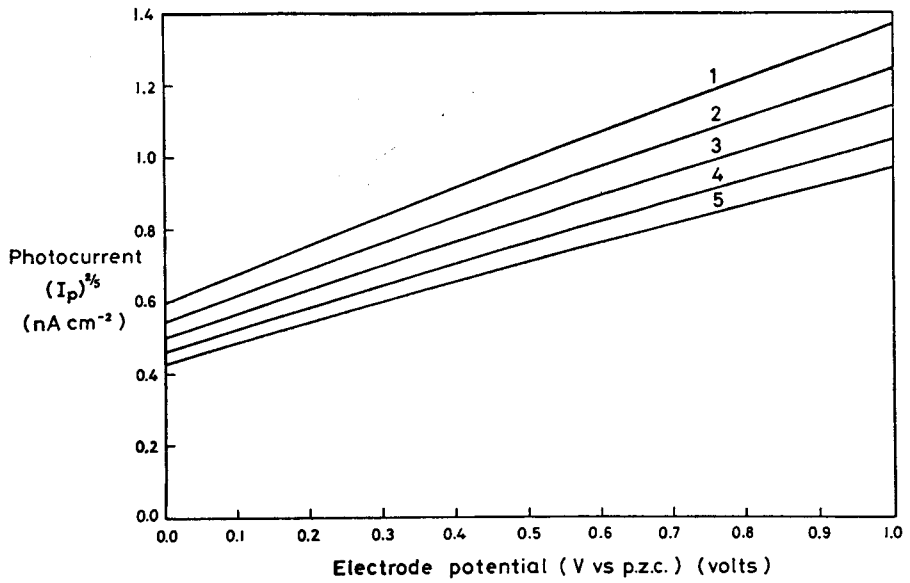

Fig. 8. The dependence of 2/5th power of the photocurrent on electrode potential for electron transfer from a mercury electrode to acceptors in the electrolyte for photon energy, $h\nu = 3.5$ eV and for different barrier heights U_m. Curve 1, for $U_m = 13.8$ (1.0 eV less than the calculated $U_m = 14.8$ eV). Curve 2, for $U_m = 14.3$ eV. Curve 3, for $U_m = 14.8$ eV (calculated value). Curve 4, for $U_m = 15.3$ eV and curve 5, for $U_m = 15.8$ eV (1.0 eV more than the calculated $U_m = 14.8$ eV).

Photocurrents were calculated using eq. (33) for radiation energy $h\nu=$ 3.5 eV for arbitrary values of barrier heights from 1.38 eV to 15.8 eV, and it was observed that, in such a range of the values of U_m, the theory gives rise to the 5/2 law, and the variation of the threshold energy in this range of the U_m (± 1 eV) is negligible (Fig. 8 and Table 5).

TABLE 5. The threshold energy $h\nu_0$ (extrapolated) for different barrier height, U_m

Photon energy $h\nu$ in eV	Barrier height U_m in eV	Extrapolated threshold energy $h\nu_0$ in eV (from eq. (33))	Remarks
3.5	13.8	2.8	Negligible change in threshold energy $h\nu_0$ with change of barrier height U_m by ± 1 eV
	14.3	2.85	
	14.8*)	2.85	
	15.3	2.85	
	15.8	2.9	

*) The calculated value of U_m.

The present model takes into account the variation of the depth of penetration with the energy of the radiation, the effect of absorbance and reflectivity of light by different electrode materials, and the effect of electron-electron and electron-phonon scattering length of electrons in metals, on photocurrents. It also gives some account of the angular distribution of outcoming photoexcited electrons from within the metal bulk.

10. Non-Tafel Behaviour of the Photocurrent

It is well known that electrochemical dark currents follow Tafel's law, but one observes that the photocurrent does not follow it (Fig. 9).

There is a Boltzmann type of distribution of acceptor states in solution. For the hydrogen evolution at the cathode, one finds that the ground state of the acceptor is at 3.0 eV above the Fermi level of the Hg-electrode (see Section 5). The distributed higher energy states are close to Fermi levels, their number is reduced exponentially from the ground state and is given by[33]

$$N(E) = N_0 \exp\left\{-\beta(E_g - E)/kT\right\} \tag{35}$$

where N_0 is the number of acceptors at its ground state.

Correspondingly, dark current electrons come from the Fermi level, because, even if the potential is as high as 2 volts (*vs.* the *p. z. c.*), the

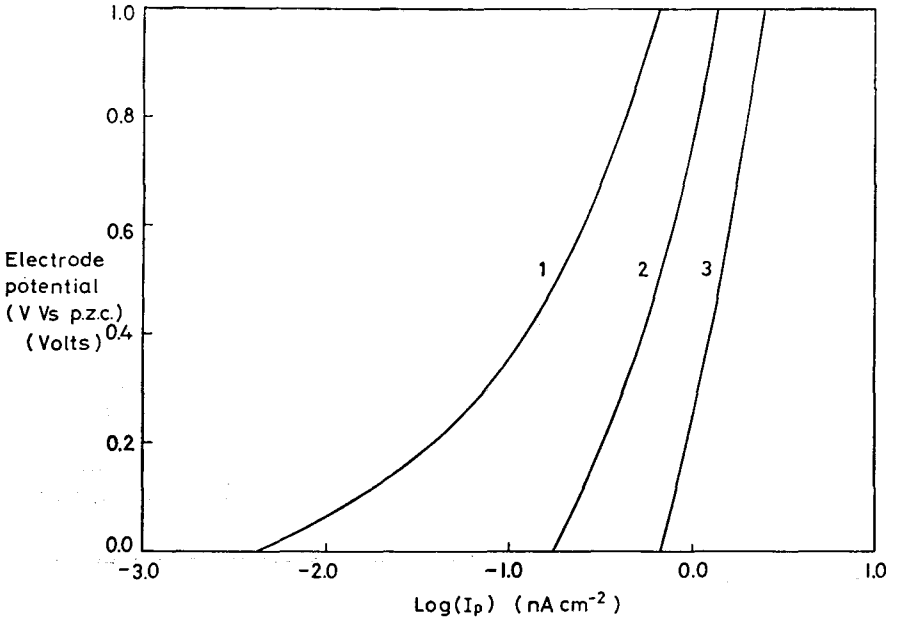

Fig. 9. The dependence of the logarithm of the photocurrent, I_p, on the electrode potential (shows non-Tafelian behaviour). Curve 1, for $h\nu=3.0$ eV. Curve 2, for $h\nu=3.5$ eV. Curve 3, for $h\nu=4.0$ eV.

Fermi level is still below the ground state of the acceptor, H_3O^+ ions so that the electrons go to it and not to the solvent state. As the acceptor states are classically distributed in solution one gets an exponential behaviour of the dark current with potential (since in eq. (35), $E=E_f-e_0V$) and, therefore, the logarithmic Tafel law is followed.

For photocurrents the photon energy is such that the Fermi electrons can be excited above the ground state of the acceptor (Fig. 3). The major contribution to the photocurrent is then due to the photoelectrons which tunnel through the potential barrier, and go to *solvent* states above the energy of the H_3O^+ states. The number of these states per unit area is not distributed Boltzmannianly because the energy concerned is *total*, not potential energy, and the states concerned are not bound states. Thus, photocurrents do not depend on the availability of exponentially distributed vibration-rotational states in H_3O^+, and accordingly do not follow Tafel's law for the exponential dependence of current on potential.

11. Limitations of the Present model

The present model has not been applied to find certain secondary effects such as the dependence of I_p on the angle of incidence, the plane of polarisation of the radiation[34], and the effect of different crystal faces[35] of the electrode. It cannot be used to interpret anodic photocurrents in its present form.

Acknowledgements

The authors thank Dr. K. GOPALSAMY and Mr. P. WRIGHT of The Flinders University for mathematical discussions.

References

1) P. E. CLARK and A. B. GARRETT, J. Am. Chem. Soc., **61**, 1805 (1939).
2) A. W. COPELAND, O. D. BLACK and A. D. GARRETT, Chem. Rev., **31**, 177 (1942).
3) P. J. HILLSON and E. K. RIDEAL, Proc. Roy. Soc. London, **199**, 295 (1949).
4) G. C. BARKER, A. W. GARDNER and D. C. SAMMON, J. Electrochem. Soc., **113**, 1183 (1966).
5) M. HEYROVSKÝ, Proc. Roy. Soc. London, **A 301**, 411 (1967).
6) R. DE LEVIE and J. E. KRENSER, J. Electroanal. Chem., **21**, 221 (1969).
7) YU. V. PLESKOV and Z. A. ROTENBERG, J. Electroanal. Chem., **20**, 1 (1969).
8) L. I. KORSHUNOV, YA. M. ZOLOTOVITSKII and V. A. BENDERSKII, Russ. Chem. Rev. **40**, 699 (1971).
9) V. I. VESELOVSKII, Zhur. Fiz. Khim., **20**, 1493 (1946).
10) N. H. FOWLER, Phys. Rev., **38**, 45 (1931).
11) L. A. DUBRIDGE, Phys. Rev., **29**, 108 (1932).
12) G. W. WEDLER, C. WOFING and P. WIESSMANN, Surface Sci., **24**, 302 (1971).
13) A. M. BRODSKII, YU. YA. GUREVICH, Zh. Eksperim. Teor. Fiz., **54**, 213 (1968).
14) D. B. MATTHEWS and S. U. M. KHAN, Aust. J. Chem., **28**, 253 (1975).
15) A. J. APPLEBY, J. O'M. BOCKRIS and A. K. SEN and B. E. CONWAY, *M. T. P. International Review of Science*, ed. J. O'M. BOCKRIS, Vol. **6**, Butterworth, London, 1973.
16) F. CONSTANTINESCU, E. MAGYARI, *Problems in Quantum Mechanics*, Pergamon Press, Oxford, 1971.
17) J. O'M. BOCKRIS and A. K. N. REDDY, *Modern Electrochemistry*, Vol. **2**, Plenum Press, New York, 1973.
18) R. A. MARCUS, (a) J. Chem. Phys., **24**, 966 (1956); (b) J. Chem. Phys., **43**, 679 (1965).
19) V. G. LEVICH, *Physical Chemistry, An Advanced Treatise*, ed. H. EYRING, D. HENDERSON and W. JOST, Vol. **IXB**, Acad. Press, New York, 1971.
20) P. P. SCHMIDT, J. Phys. Chem., **77**, 488 (1973).
21) K. FUEKI, D. F. FENG and L. KEVAN, J. Phys. Chem., **74**, 1976 (1970).

22) C. KETTEL, *Introduction to Solid State Physics*, 4th edition, Wiley and Sons, New York, 1971.
23) H. MARGENAU and W. G. POLLARD, Phys. Rev., **60**, 128 (1941).
24) R. GOMER, *Photo-field Emission Ionization*, Oxford Univ. Press, London, 1961.
25) D. PENN, R. GOMER and M. H. COHEN, Phys. Rev. Lellers, **27**, 26 (1971).
26) J. W. GUDZAK, Phys. Rev., **1**, 2110 (1970).
27) J. O'M. BOCKRIS and D. B. MATTHEWS, Proc. Roy. Soc., London, **A 292**, 479 (1966).
28) S. TRASATTI, J. Electroanal. Chem., **52**, 313 (1974).
29) A. BEN-NAIM and F. H. STILLINGER, *Structure and Processes in Water and aqueous Solutions*, ed. R. A. HORNE, Wiley, New-York, 1971.
30) J. VALASEK, *International Critical Tables*, Vol. **VI**, 248 (1929).
31) P. KROLIKOWSKI and W. E. SPICER, Phys. Rev., **185**, 882 (1969).
32) H. KANTER, Phys. Rev., **1**, 522 (1970).
33) R. GURNEY, Phys. Rev., **A 34**, 137 (1931).
34) N. M. BRONDY, Phys. Rev., **3**, 364 (1971).
35) N. V. SMITH, C.N.C. Critical, Rev. Solid State Sci., **45**, 1 (1971).